International Refereed Journal of Engineering and Science (IRJES)
ISSN (Online) 2319-183X, (Print) 2319-1821
Volume 2, Issue 12 (December 2013), PP. 08-17

Fault Ride Through of a Dfig Wind Turbine Using Dvr with Modified Control Scheme

Harikrishna Parsa[1], Dr.Narasimham R.L[2]
[1]*PG-Scholar, Dept. of Electrical And Electronics, TKR Engg. College, Hyderabad, India*
[2]*Prof and Dean (RPD), Dept. of Electrical And Electronics, TKR Engg. College, Hyderabad, India*

Abstract:- This paper presents the application of a Dynamic Voltage Restorer (DVR) connected to a wind turbine driven Doubly Fed Induction Generator (DFIG) is investigated. This setup allows the wind turbine system an uninterruptible fault ride-through of voltage dips. The DVR can compensate the faulty line voltage, while the DFIG wind turbine can continue its nominal operation as demanded in actual grid codes. Simulation results for a 2 MW wind turbine are presented, especially for asymmetrical grid faults. They show the effectiveness of the DVR in comparison to the low-voltage ride-through of the DFIG using a crowbar that does not allow continuous reactive power production. A modified control scheme for the DVR will improve the fault ride through behavior of the wind turbine in terms of harmonics and settling time.

Keywords:- Doubly Fed Induction Generator (DFIG), Dynamic Voltage Restorer (DVR), Fault Ride Through , Voltage sag.

I. INTRODUCTION

With the increase of grid connected power generation from the wind energy systems, fault ride through capability is demanded for Doubly Fed Induction Generator (DFIG) to decrease the adverse effect on stability of power system. Fault ride through (FRT) refers the operation during grid voltage faults, wind turbines must stay connected to the grid and should support the grid by generating reactive power to support and restore quickly the grid voltage after the fault. A detailed analysis has given in [1].

It requires grid code requirements to maintain a stable and safe operation of the power system network. The actual grid codes stipulate that wind farms should contribute to power system control like frequency and voltage to behave similar to conventional power stations. A detailed review of grid code technical requirements regarding the connection of wind farms to the electrical power system is given in [2]. Among wind turbine concepts, turbines using the DFIG are dominant due to its variable-speed operation, its separately controllable active and reactive power, and its partially rated power converter. But there are some issues should be concerned when the wind farms with DFIGs are connected to the grid.

(1) Power quality induced by fluctuant power
(2) Operation of DFIG during grid faults

But the reaction of DFIGs to grid voltage disturbances is sensitive i.e., faults far away from the location of the turbine can cause a voltage dip at the connection point of the wind turbine. The dip in the grid voltage will result an increase of the current in the stator windings of DFIG, which will induce the over current in the rotor circuit and the power electronic converter. To improve the Low Voltage Ride through (LVRT) capability of wind farms several approaches have been proposed. They can be divided into three categories.

(1) Improvement of the control of the power converter,
(2) Installation of additional hardware and
(3) Determination of the optimal Point of Common Coupling (PCC).

Conventionally, a resistive network called Crowbar is connected in case of rotor over currents or DC-link over voltages to the rotor circuit, and the rotor side converter (RSC) is disabled. But the machine draws a high short circuit current when the Crowbar is activated, resulting in a large amount of reactive power drawn from the power network, which is not acceptable when considering actual grid code requirements. Thus, other protection methods have to be investigated to ride-through grid faults safely and fulfill the grid codes.

There are other proposed solutions using additional hardware for fault ride-through of a DFIG using additional hardware like a series dynamic resistance in the rotor or in the stator or using a series Line Side Converter (LSC) topology as in [3]. Other approaches focus on limiting the rotor currents during transient grid voltage by changing the control of the RSC in order to avoid additional hardware in the system. The RSC can be protected by feed forward of the faulty stator voltage, by considering the stator flux linkage or by using the measured stator currents as reference for the rotor current controllers [4]. Other publications focus on the improved performance during unsymmetrical grid voltage conditions. A demagnetizing current is used to

protect the converter in, but it becomes clear that during deep transient dips, Crowbar activation cannot be avoided, and thus, continuous reactive power control cannot be guaranteed.

If an external power electronic device is used to compensate the faulty grid voltage, any protection method in the DFIG system can be left out. Such a system is introduced in this paper i.e., dynamic voltage restorer (DVR) that is a voltage source converter connected in series to the grid to correct faulty line voltages. The advantages of such an external protection device are thus the reduced complexity in the DFIG system. The disadvantages are the cost and complexity of the DVR. Note that a DVR can be used to protect already installed wind turbines that do not provide sufficient fault ride-through behavior or to protect any distributed load in a micro grid. Control structures based on resonant controllers to compensate unsymmetrical voltages are presented.

In this paper, the application of a DVR that is connected to a wind-turbine-driven DFIG to allow uninterruptible fault ride through of voltage dips fulfilling the grid code requirements is investigated. The DVR can compensate the faulty line voltage, while the DFIG wind turbine can continue its nominal operation as demanded in actual grid codes. Here, asymmetrical faults are investigated; detailed analysis of DFIG behavior and DVR control is given here.

The understanding of rotor over currents during symmetrical grid voltage dip using a DFIG wind turbine is described in Section II. Only if the RSC can provide a sufficient voltage level, controllability of rotor currents can be obtained. If the rotor voltage exceeds the converter voltage, high currents will flow through the diodes into the dc-link capacitor, damaging the Insulated Gate Bipolar Transistor (IGBT) or the DC capacitor. An analysis of rotor voltage dynamics during transient symmetrical voltage dip and a description of the control structure and conventional crowbar protection are given. The DVR electrical system and control using controllers are described in Section III. Simulation results for a 2MWwind turbine in Section IV show the effectiveness of the proposed technique in comparison to the low-voltage ride-through of the DFIG using a Crowbar. A conclusion closes the analysis.

II. DOUBLY FED INDUCTION GENERATOR

2.1 Introduction

In variable-speed wind turbine with full converter, the generator can be a squirrel-cage induction or a synchronous generator which is connected to the grid via a power electronic converter as shown in Fig.1 The whole power output from generator goes through the converter and therefore the converter is rated at full power. Among wind turbine concepts, turbines using DFIG are described in [5].

A power electronic converter is used in the variable-speed wind turbine with doubly fed induction generator as shown in Fig.2. The converter is connected to the generator rotor and the stator is directly connected to the grid. Compared to the one with full converter, this type is more suitable for high power wind turbines since only a fraction (typically 20-30%) of the total power goes through the converter. This gives possibility to design the converter with smaller size, and as a result, lower cost and lower power electronic losses.

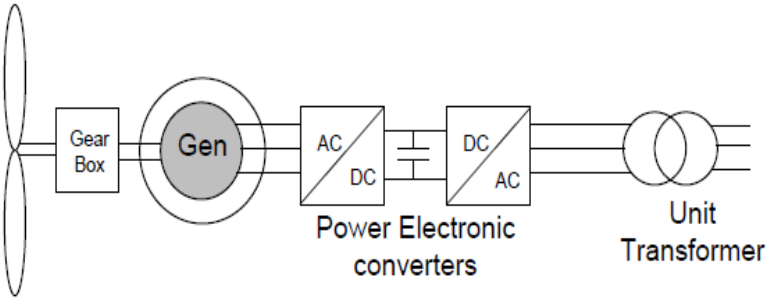

Fig.1. Full converter wind turbine

The investigated wind turbine system, as shown in Fig. 2, consists of the basic components like the turbine, a gear (in most systems), a DFIG, and a back-to-back voltage source converter with a DC link. A dc chopper to limit the dc voltage across the dc capacitor and a crowbar are included. The back-to-back converter consists of a RSC and a LSC, connected to the grid by a line filter to reduce the harmonics caused by the converter. A DVR is included to protect the wind turbine from voltage disturbances. Due to the short period of time of voltage disturbances, the dynamics of the mechanical part of the turbine will be neglected and the mechanical torque brought in by the wind is assumed to be constant.

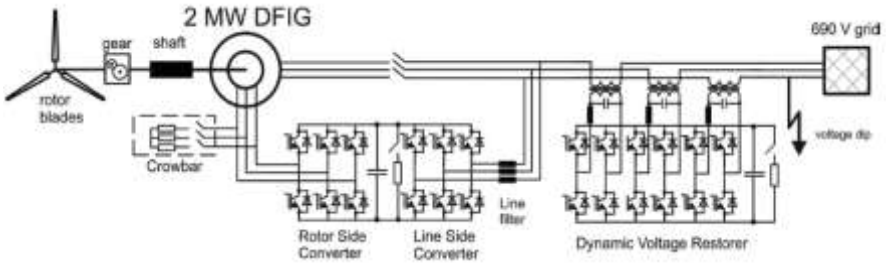

Fig.2. Schematic diagram of DFIG wind turbine system with DVR.

2.2 Rotor Voltage Dynamics

A precise knowledge about amplitude and frequency of the rotor voltage is necessary to design and control the RSC. Therefore, equations for the rotor voltage in normal operation and under symmetrical stator voltage dip are derived in the following. Afterwards, the rotor converter rating is taken into account.

From the per-phase equivalent circuit of the DFIG in a static stator- oriented reference frame, the following stator and rotor voltage and flux equations can be derived:

$$\vec{v}_s = R_s\vec{i}_s + \frac{d\vec{\psi}_s}{dt} \quad \text{..... (1)}$$

$$\vec{v}_r = R_r\vec{i}_r + \frac{d\vec{\psi}_r}{dt} - j\Omega\vec{\psi}_r \quad \text{.....(2)}$$

$$\vec{\psi}_s = L_s\vec{i}_s + L_h\vec{i}_r \quad \text{.....(3)}$$

$$\vec{\psi}_r = L_r\vec{i}_r + L_h\vec{i}_s \quad \text{..... (4)}$$

Where $\vec{\psi}$, $\vec{v}$, and $\vec{i}$ represent the flux, voltage, and current vectors, respectively. Subscripts *s* and *r* denote the stator and rotor quantities, respectively. $L_s = L_{s\sigma} + L_h$ and $L_r = L_{r\sigma} + L_h$ represent the stator and rotor inductance, L_h is the mutual inductance, R_s and R_r are the stator and rotor resistances, and Ω is the electrical rotor frequency.

By introducing the leakage factor $\sigma = 1 - (L_h^2/L_sL_r)$, the rotor flux can be described in dependence of the rotor current and the stator flux

$$\vec{\psi}_r = \frac{L_h}{L_s}\vec{\psi}_s + \sigma L_r\vec{i}_r \quad \text{..... (5)}$$

By substituting (5) in (2), an equation for the rotor voltage can be obtained

$$\vec{v}_r = \frac{L_h}{L_s}\left(\frac{d}{dt} - j\Omega\right)\vec{\psi}_s + \left(R_r + \sigma L_r\left(\frac{d}{dt} - j\Omega\right)\right)\vec{i}_r \quad \text{.... (6)}$$

which consists of two parts. The first part is caused by the stator flux $\vec{\psi}s$ that is given in normal operation by the constantly rotating vector

$$\vec{\psi}_s = \frac{V_s}{j\omega_s}e^{j\omega_s t} \quad \text{..... (7)}$$

The second part of (6) is caused by the rotor current $\vec{i}_r$. The rotor resistance R_r and the leakage factor σ are often small, so the rotor voltage does not differ considerably from the part caused by the stator flux. Thus, the amplitude of the rotor voltage in normal condition V_{r0} can be calculated as

$$V_{r0} \approx V_s\frac{L_h}{L_s}\frac{\omega_r}{\omega_s} = V_s\frac{L_h}{L_s}s \quad \text{..... (8)}$$

where $s = 1 - (\Omega/\omega_s) = \omega_r/\omega_s$ describes the slip and ω_r the slip frequency. The rotor voltage induced by the stator flux increases the most during a full symmetrical stator voltage dip. Under a symmetrical voltage dip, the stator voltage is reduced from normal amplitude V_1 to the faulty amplitude V_2 as described in (9)

$$\vec{v}_s = \begin{cases} V_1 e^{j\omega_s t} & for\ t \le t_0 \\ V_2 e^{j\omega_s t} & for\ t \ge t_0 \end{cases} \quad \text{..... (9)}$$

$$\vec{\psi}_s = \begin{cases} \vec{\psi}_{s1} = \frac{V_1}{j\omega_s}e^{j\omega_s t}, & for\ t \le t_0 \\ \vec{\psi}_{s2} = \frac{V_2}{j\omega_s}e^{j\omega_s t}, & for\ t \ge t_0 \end{cases} \quad \text{..... (10)}$$

Since the stator flux is a continuous value, it cannot follow the step function of the voltage. The evolution of the stator flux can be derived by solving the differential equation (11) (from (1) and (3), assuming $\vec{i}_r = 0$ due to its low influence on the rotor voltage)

$$\frac{d\vec{\psi}_s}{dt} = \vec{v}_s - \frac{R_s}{L_s}\vec{\psi}_s \quad (11)$$

The solution consists of two parts. The first part is the steady state stator flux after the voltage dip that is described by $\vec{\psi}_{s2}$ and the second part is the transition of the flux from $\vec{\psi}_{s1}$ to $\vec{\psi}_{s2}$ that is described by (12)

$$\vec{\psi}_s = \vec{\psi}_{s0}\, e^{-tRs/Ls} = \vec{\psi}_{s0}\, e^{-t/\tau_s} \quad (12)$$

where $\vec{\psi}_{s0}$ is the difference of the stator flux before and after the voltage dip, described by $(V_1 - V_2)/j\omega_s$. Summarizing, the stator flux is given by the sum of the two parts

$$\vec{\psi}_s(t) = \frac{V_2}{j\omega_s} + \frac{V_1 - V_2}{j\omega_s} e^{-t/\tau_s} \quad (13)$$

When the dynamic stator flux from (13) is considered in the rotor voltage equation of (6) (neglecting $\vec{i}_r$ and $1/\tau_s$), the dynamic behavior of the rotor voltage under symmetrical voltage dip is described by (15)

$$\vec{v}_r = \frac{L_h}{L_s}\left(\frac{d}{dt} - j\Omega\right)\left(\frac{V_2}{j\omega_s} e^{j\omega_s t} + \frac{V_1 - V_2}{j\omega_s}\, e^{-t/\tau_s}\right) \quad (14)$$

$$= \frac{L_h}{L_s}\left(sV_2\, e^{j\omega_s t} - (1 - s)(V_1 - V_2)e^{-t/\tau_s}\right) \quad (15)$$

In a reference frame rotating at rotor frequency, the following rotor voltage is obtained:

$$\vec{v}_r = \frac{L_h}{L_s}\left(sV_2\, e^{j\omega_r t} - (1 - s)(V_1 - V_2)e^{-j\Omega t}\, e^{-t/\tau_s}\right) \quad (16)$$

The results of this analysis show that the rotor voltage during symmetrical voltage dip consists of two components. The first part is proportional to the slip and the remaining stator voltage; thus, for a deep voltage dip and a slip usually at − 0.2, it is small. The frequency of the first part is the slip frequency (at a slip of − 0.2, ω_r = 10Hz). The second part of (16) has a high amplitude at t = 0 proportional to (1 − s) and rotates at the electrical rotor frequency Ω (at a slip of −0.2, Ω = 60Hz). The part is decaying exponentially with the stator time constant of τ_s. The maximum rotor voltage during symmetrical voltage dip will occur at the beginning of the fault (t = 0) and for a full dip (V_2 = 0)

$$V_{r,\max} \approx \frac{L_h}{L_s}(1 - s)V_1 \quad (17)$$

Note that (17) is an approximation of the maximum rotor voltage under the given circumstances. The RSC of a DFIG is rated for a part of the stator power, because the rotor power is approximately proportional to the slip $P_r \approx sP_s$ that is chosen usually between ±0.3. The required amplitude of the rotor voltage is probably determined [with $L_h/L_s \approx 1$ in (8)] by

$$V_r = \frac{sV_s}{N_{sr}} \quad (18)$$

where N_{sr} is the stator to rotor turns ratio. The turn's ratio is usually set at 1/2 or 1/3 in practical wind-turbine-driven DFIGs to make full use of the dc-link voltage and reduce the converters current rating. The required dc-link voltage can be determined by

$$m\frac{V_{dc}}{2} = V_r \quad (19)$$

where m is the modulation index of the pulse width modulation (PWM) technique. The value of the modulation index is 1.0 for the carrier-based sinusoidal PWM and 1.15 for the space vector modulation, both without over modulation techniques. The findings of the section enhance the understanding of rotor over currents during symmetrical grid voltage dip. Only if the RSC can provide a sufficient voltage level, controllability of rotor currents can be obtained. If the rotor voltage exceeds the converter voltage, high currents will flow through the diodes into the dc-link capacitor, damaging the insulated gate bipolar transistor (IGBT) or the dc capacitor.

2.3 RSC Control

The RSC provides decoupled control of stator active and reactive power. A cascade vector control structure with inner current control loops is applied. The overall control structure is shown in Fig. 3. When adopting stator-voltage-oriented (SVO) control, a decomposition in d and q components is performed (V_{sq} = 0). Neglecting the stator resistive voltage drop, the stator output active and reactive powers are expressed as

$$P_s \approx \frac{3}{2}\frac{L_h}{L_s} V_{sd}\, I_{rd} \quad (20)$$

$$Q_s \approx -\frac{3}{2}\frac{V_{sd}}{L_s}\left(\frac{L_{sd}}{\omega_s} + L_h I_{rq}\right) \quad \text{..... (21)}$$

thus, the stator active and reactive power can be controlled independently, controlling the *d* and *q* components of the rotor current. Based on (20) and (21), the outer power control loops are designed.

2.4 LSC Control

The LSC controls the dc voltage V_{dc} and provides reactive power support. A voltage-oriented cascade vector control structure with inner current control loops is applied [see Fig. 3 (right)]. The line current I_l can be controlled by adjusting the voltage drop across the line inductance L_l giving the following dynamics:

$$V_s = R_l I_l + L_l \frac{dI_l}{dt} \quad \text{..... (22)}$$

which is used to design the current controller, while the dc voltage dynamics can be expressed by

$$C_{dc}\frac{dV_{dc}}{dt} = I_{dc} - I_{load} \quad \text{..... (23)}$$

which is used to design the outer dc voltage control loop, where C_{dc} is the dc capacitance and I_{dc} and I_{load} are the dc currents on LSC and RSC side, respectively.

2.5 Crowbar Protection

To protect the RSC from tripping due to over currents in the rotor circuit or overvoltage in the dc link during grid voltage dips, a crowbar is installed in conventional DFIG wind turbines, which is a resistive network that is connected to the rotor windings of the DFIG. The crowbar limits the voltages and provides a safe route for the currents by bypassing the rotor by a set of resistors. When the crowbar is activated, the RSCs pulses are disabled and the machine behaves like a squirrel cage induction machine directly coupled to the grid. The magnetization of the machine that was provided by the RSC in nominal condition is lost and the machine absorbs a large amount of reactive power from the stator, and thus, from the network, which can further reduce the voltage level and is not allowed in actual grid codes. Triggering of the crowbar circuit also means high stress to the mechanical components of the system as the shaft and the gear. Detailed analyses on the DFIG behavior during voltage dip and crowbar protection can be found. Thus, from network and machine mechanical point of view, a crowbar triggering should be avoided. Anyway, to compare the presented technique here with a conventional DFIG wind turbine system protected by a crowbar circuit, simulation results including crowbar protection are examined. Therefore, the crowbar resistance is designed here.

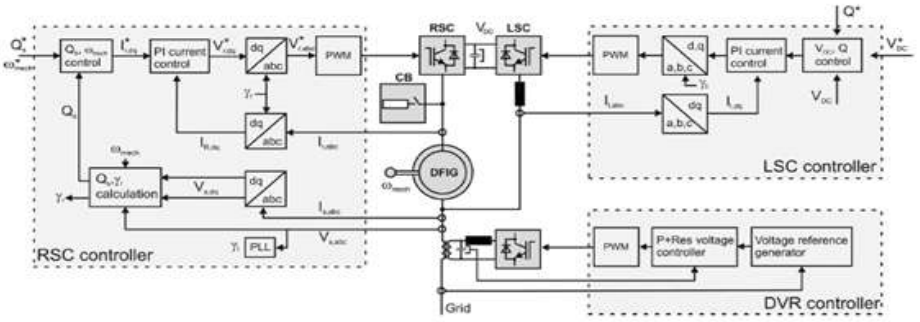

Fig.3. Schematic diagram of DFIG wind turbine and DVR control structure.

There are two constraints that give an upper and a lower limit to the crowbar resistance. As a first constraint, the crowbar resistance should be high enough to limit the short-circuit rotor current $I_{r,max}$. As the second constraint, the crowbar resistance should be low enough to avoid too high voltage in the rotor circuit. If the rotor phase voltage across the crowbar rises above the maximum converter voltage given in (18), high currents will flow through the anti parallel diodes of the converter. A crowbar resistance of $R_{crow} = 150R_r$ is used in the simulations. There are approaches limiting the operation time of the crowbar to return to normal DFIG operation with active and reactive power control as soon as possible by injecting a demagnetizing current or using a threshold control.

III. DYNAMIC VOLTAGE RESTORER

3.1 Introduction

Dynamic Voltage Restorer (DVR) in the literature as their primary application is to compensate for voltage sags and swells. Their configuration is similar to that of SSSC. However, the control techniques are different. Also, a DVR is expected to respond fast (less than 1/4 cycle) and thus employs PWM converters using IGBT devices.

The most common disturbances in the source voltages are the voltage sags or swells that can be due to (i) disturbances arising in the transmission system, (ii) adjacent feeder faults and (iii) fuse or breaker operation. Voltage sags of even 10% lasting for 5-10 cycles can result in costly damage in critical loads. The voltage sags can arise due to symmetrical or unsymmetrical faults. In the latter case, negative and zero sequence components are also present. Uncompensated nonlinear loads in the distribution system can cause harmonic components in the supply voltages. To mitigate the problems caused by poor quality of power supply, series connected compensators are used.

Fast variations in the source voltage cannot be ignored, these can affect the performance of critical loads such as (a) semiconductor fabrication plants (b) paper mills (c) food processing plants and (d) automotive assembly plants.

3.2 Electrical System

A DVR is a voltage source converter equipped with a line filter (usually *LC* type). Usually, a coupling transformer is used in series to the grid in order to correct deteriorated line voltages to reduce possible problems on a sensitive load or generator. Different transformer-based topologies are compared with respect to the number of hardware components, switching harmonics, dc-link control, and the ability to inject zero sequence voltages. Different system topologies are investigated in regard to the connection of the dc link and the rating in power and voltage. The rating of the DVR system depends mainly on the depth of the voltage fault that should be compensated. For voltage sags or swells with zero-phase angle jump, the requirement of active power of the DVR is simply given by

$$P_{DVR} = \left(\frac{V_1 - V_2}{V_1}\right) P_{load} \quad \text{..... (24)}$$

where V_1 is the nominal and V_2 the faulty line voltage. Note that special focus must be taken on voltage faults with phase angle jump that can lead to a higher power rating. When the DVR compensates a voltage sag, the active power of the DFIG is partly fed into the grid and the DVR system that is dependent of the remaining grid voltage. The active power flowing into the DVR charges its dc link. The excess energy must either be delivered to an energy storage system or transformed into heat by a dc chopper. Note that for full compensation of a full voltage dip, the DVR must be rated for the power of the wind turbine, making the solution in economical. Thus, the solution will probably be implemented to fully compensate the line voltage during partial voltage dip or swell and to assist during full voltage dip. The injection transformers have a great impact on the DVR design. To adapt the DVR dc voltage to the compensating voltage, an adequate transformer ratio must be chosen. The design of the injection transformers differs from normally used shunt transformers. They must be higher rated to avoid possible saturation effects and lower the risk of high inrush currents that must be handled by the converter. In practical applications, several security issues must be considered. Since the DVR is connected in series to the load, bypass switches across the transformers must be included to disconnect the DVR from the load, to protect the converter from damage in overload situations.

3.3 DVR Control

For control of the DVR system, a closed-loop control in a rotating *dq* reference frame is introduced in, but identified as unsuitable for the compensation of unsymmetrical grid faults. Because the majority of faults on a power system are unbalanced in nature, which results in unbalanced voltages, appropriate generation of unsymmetrical compensation voltage components by the DVR is an important feature. Thus, stationary-frame controllers for DVR implementation are designed to achieve good positive- and negative-sequence voltage regulation. The cascade control structure includes inner proportional current controllers. As outer voltage controllers proportional + resonant (P+Res) controllers are compared to *H*∞-controllers. Both control structures have good steady-state sinusoidal error tracking of the positive- and negative-sequence voltage components. Anyway, DVR current control is inadequate if the load is current-controlled too. Therefore, P+Res voltage controllers that are controlling directly the voltage across the filter capacitors without inner current controllers are used here. The controller transfer function expressed in terms of inverter voltage reference u^*_i , measured filter capacitor voltage uc , and filter capacitor voltage reference u^*c is given by

$$u_i^*(s) = u_c(s) + G_{p+Res}(s) \cdot (u_c^*(s) - u_c(s)) \quad \text{.....(25)}$$

where a feed forward of the measured filter capacitor voltage is used. The transfer function of the P+Res voltage controller is defined as

$$G_{P+Res}(s) = K_P + K_I \frac{s}{s^2 + \omega_0^2} \quad \text{..... (26)}$$

which has been implemented in the discrete form leading to the following transfer function:

$$G_{P+Res}(z) = K_P + K_I \frac{zT_s - T_s}{z^2 + z\left(T_s^2 \omega_0^2 - 2\right) + 1} \quad \text{..... (27)}$$

Additionally, an anti windup functionality has been added. The control parameters K_P and K_I were found by the analysis of bode plots and root loci of the given discrete controller. The inverter system has been

discrete modeled consisting of a delay element in series with the transfer function of the *LC* line filter. The proposed fuzzy control structure is shown in the following figure.

3.4 Proposed Method

The fuzzy control of DVR will improve the performance is achieved with negligible amount of spikes and reach the steady state with less time. Thus the proposed Fuzzy Control (FC) has better dynamic behavior than conventional PI Control. The centroid method is employed for defuzzification. For the proposed FC, the input signals are error and change in error are properly scaled and fuzzified. Seven membership functions are used for error, change in error. A rule table relating each one of the 49 input label pairs to respective output label is shown in above Table 1.

Table 1: Fuzzy rule representation

ΔE **e**	**NB**	**NM**	**NS**	**Z**	**PS**	**PM**	**PB**
NB	NB	NB	NB	NB	NM	NS	Z
NM	NB	NB	NB	NM	NS	Z	PS
NS	NB	NB	NM	NS	Z	PS	PM
Z	NB	NM	NS	Z	PS	PM	PB
PS	NM	NS	Z	PS	PM	PB	PB
PM	NS	Z	PS	PM	PB	PB	PB
PB	Z	PS	PM	PB	PB	PB	PB

IV. RESULTS AND ANALYSIS

Detailed simulation studies carried out on MATLAB/Simulink platform to verify the operating behavior of the proposed scheme as shown in fig.2 modeled in Simulink is shown in fig.4. Machine parameters chosen for carrying out the simulation study are provided in Table 2.

Table 2 Simulation Parameters

Simulation Parameters		
Symbol	Quantity	Value
U_{line}	low voltage level (phase-to-phase, rms)	690 V
ωs	Line angular frequency	2π 50 Hz
P_{DFIG}	Wind turbine rated power	2 MW
i	Stator to rotor transmission ratio	1
n	Rated mechanical speed	1800 r/min
L_h	mutual inductance	3.7 mH
Rs	stator resistance	10mΩ
$R_{crowbar}$	Crowbar resistance	0.3 Ω
V_{DC}	DVR DC voltage	560 V
C_{DC}	DVR DC link capacitance	7.5 mF

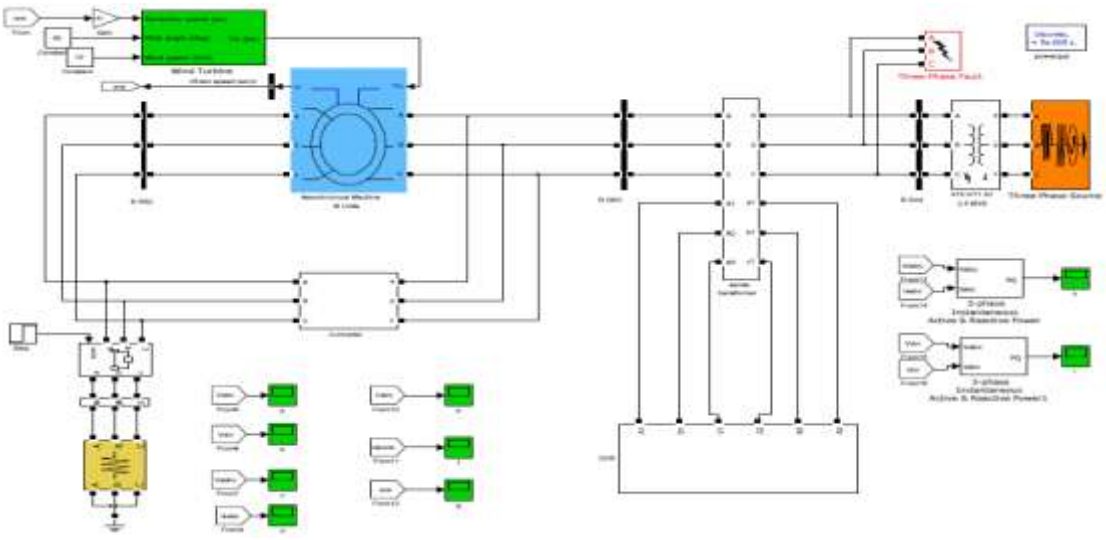

Fig.4. Simulation block diagram

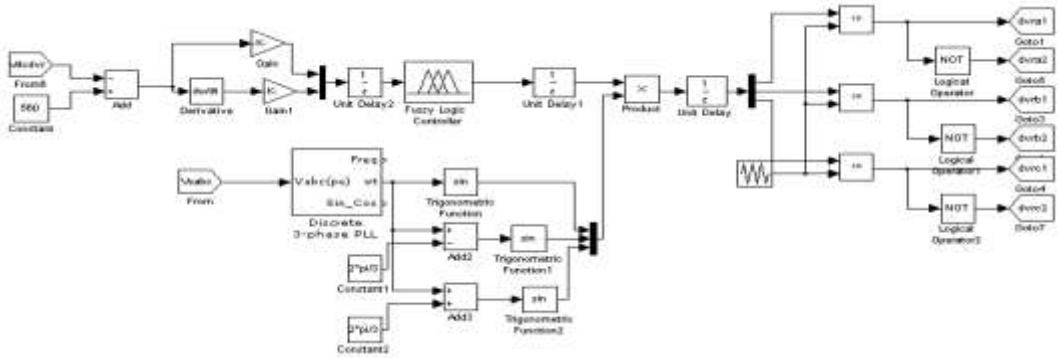

Fig.5. DVR Fuzzy control structure

The converter control and DVR control are designed with the help of control structure given in Fig.3. The DVR controlled structure is shown in Fig.5. All the simulations are done in MATLAB/Simulink version 7.8.0.347 (R2009a). On the basis of results obtained by simulation, the detailed conclusion is given.

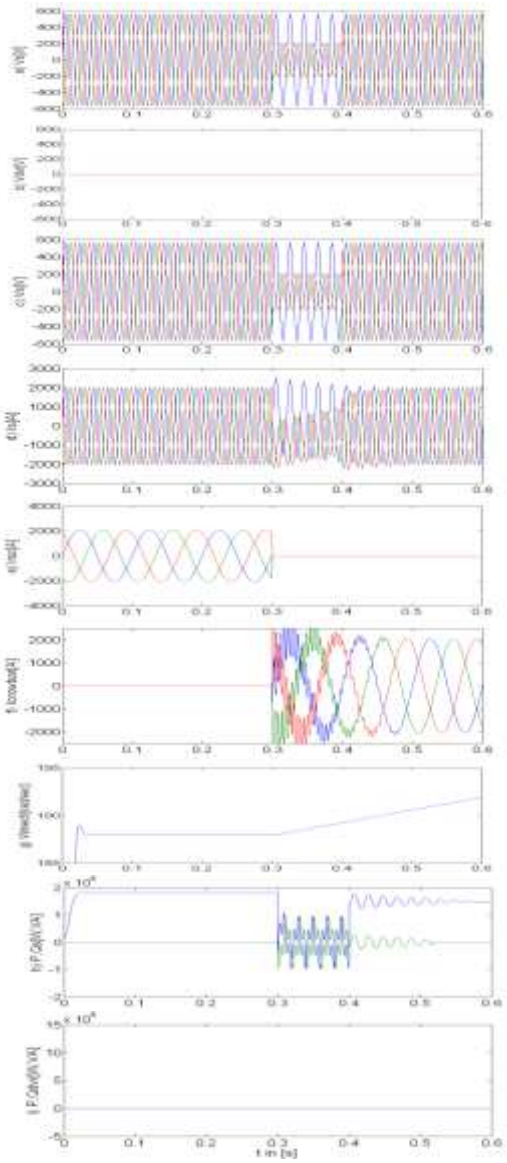

Fig.6. Simulation of DFIG performance with crowbar protection during two-phase voltage dip.

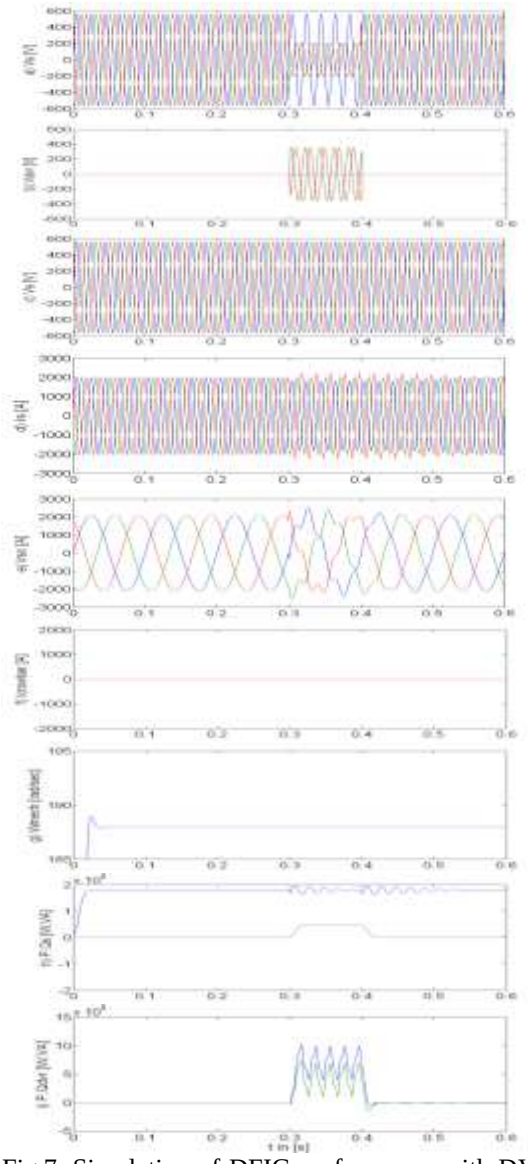

Fig.7. Simulation of DFIG performance with DVR protection during two-phase voltage dip.

(a) Line voltage. (b) DVR voltage. (c) Stator voltage. (d) Stator current. (e) RSC current. (f) Crowbar current. (g) Mechanical speed. (h) Active and reactive stator power. (i) Active and reactive DVR power.

The system performance of the DFIG is shown in Fig. 6, protected by the conventional passive crowbar, and in Fig. 7, protected by the DVR during a two-phase 37 % voltage dip of 100 ms duration [see Figs. 6(a) and 7(a)].The DFIG reacts with high stator currents *Is* , and thus, high rotor currents are induced in the rotor circuit. When the rotor currents exceed the maximum level, the crowbar is triggered to protect the RSC from over currents *I*RSC [see Fig. 6(e) and (f)]. When the voltage level has been reestablished and transients have decayed, the crowbar can be deactivated, which is not shown here. When the RSC is in operation, the machine magnetization is provided by the rotor, but when the crowbar is triggered, the RSC is disabled and the machine excitation is shifted to the stator. Thus, reactive power control cannot be provided during the voltage dip [see Fig. 6(h)], which is not acceptable when considering the grid codes. The machine cannot generate enough torque so that the rotor accelerates, which can lead to disconnection of the turbine due to over speed. The DVR is not activated in the simulations, as shown in Fig. 6. When the wind turbine system is protected by the DVR, as shown in Fig. 7, the voltage dip can almost be compensated [see Fig. 7(c)].

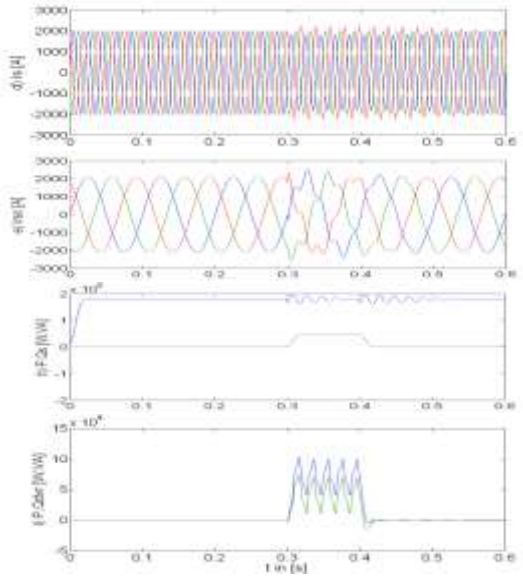

Fig.8. Simulations of DFIG performance with DVR conventional Control protection during two-phase voltage dip.

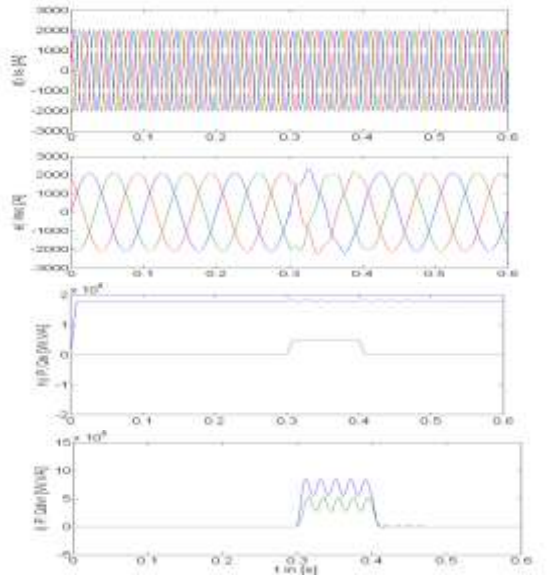

Fig.9. Simulations of DFIG performance with DVR Fuzzy control protection during two- phase voltage dip.

(d) Stator current. (e) RSC current. (h) Active and reactive stator power. (i) Active and reactive DVR power

The Fig. 8 and Fig.9 shows the comparison of outputs of the DVR control with conventional control and Fuzzy respectively. The DFIG response is much less critical, which means that lower stator over currents and rotor over currents are produced so that the crowbar does not have to be triggered [see Fig. 8(d)–(e) and 9(d)-(e)]. There is considerable reduction of over currents can be observed from the Figures 8 and 9. Note that although the stator voltage dip is fairly well-compensated, a slight distortion in the stator currents (dc components), and thus, disturbed rotor currents can be observed. Anyway, the RSC remains in operation and can control stator active and reactive power independently. Thus, the speed is kept constant and a reactive power production (*Qs* = 0.5Mvar) during grid fault as demanded in grid codes is performed. Note that a communication between DVR and DFIG is necessary. In Fig. 8(i) and 9(i), the DVR power to compensate the voltage dip is shown. It becomes clear that the active and reactive power that cannot be fed into the faulty grid during grid fault must be consumed by the DVR. The comparison of DVR control with P+Res and Fuzzy are given in Table 3 and Table 4.

Table 3 Comparison of Current level

Tolerance		
Measuring Quantity	**P+Res control**	**Fuzzy control**
Isabc(Stator Current)	2000 ± 10.5%	2000 ± 1.5%
Irabc(Rotor Current)	2000 ± 25%	2000 ± 16%

Table 4 Comparison of Settling Time

Settling time		
Measuring Quantity	**P+Res Control**	**Fuzzy control**
Isabc(Stator Current)	0.15 sec	0.1sec
Irabc(Rotor Current)	0.15 sec	0.05sec

V. CONCLUSION

Throughout this work, we have shown the effectiveness of the application of DVR control with PI and Fuzzy comparison with crowbar. In fact, the ripples are minimized in Stator side and rotor side current with the fuzzy control of DVR which we have shown in simulation. From that we will conclude that fault ride through capability is improved for wind turbine generator connected to grid. Moreover, it can also be extended to the installed wind turbines, that do not provide sufficient fault ride through behavior or to protect any distributed load in a micro grid.

ACKNOWLEDGEMENTS

I have great immense gratitude to my guide Dr.Narasimham R.L for his constant encouragement throughout this work.

REFERENCES

Journal Papers:

[1]. Chrstian Wessels, Fabian Gebhardt and Friedrich Wilhelm Fuchs. " *Fault Ride Through of DFIG Wind Turbine Using a Dynamic Voltage Restorer During Symmetrical and Asymmetrical Grid Faults*,"*IEEE Trans.Power Electron, vol.26,no.3* pp.807-815, *March 2011*.

[2]. M. Tsili and S. Papathanassiou, "*A review of grid code technical requirements for wind farms*," *Renewable Power Generat., IET*, vol. *3*, no. *3*, pp. 308–332, *Sep. 2009*.

[3]. P. Flannery and G. Venkataramanan, "*Unbalanced voltage sag ride through of a doubly fed induction generator wind turbine with series grid-side converter*," *IEEE Trans. Ind. Appl.*, vol. *45*, no. *5*, pp. 1879– 1887, *Sep./Oct. 2009.*

[4]. F. Lima, A. Luna, P. Rodriguez, E. Watanabe, and F. Blaabjerg, "*Rotor voltage dynamics in the doubly fed induction generator during grid faults*," *IEEE Trans. Power Electron.*, vol. *25*, no. *1*, pp. 118–130, *Jan. 2010*.

[5]. S.Muller,M.Deicke, and R.DeDoncker, "*Doubly fed induction generator systems for wind turbines*," *IEEE Ind. Appl.Mag.*, vol. *8*, no. *3*, pp. 26–33, *May/Jun. 2002*.